Dynamics of coupled gap solitons in diatomic lattices with cubic and quartic nonlinearities

Bambi Hu,[1,2] Guoxiang Huang,[1,3] and Manuel G. Velarde[4]
[1]Centre for Nonlinear Studies and Department of Physics, Hong Kong Baptist University, Hong Kong, China
[2]Department of Physics, University of Houston, Houston, Texas 77204
[3]Department of Physics and Laboratory for Quantum Optics, East China Normal University, Shanghai 200062, China
[4]Instituto Pluridisciplinar, Universidad Complutense, Paseo Juan XXIII, No. 1, Madrid 28040, Spain

(Received 29 November 1999)

The dynamics of coupled gap solitons in diatomic lattices with cubic and quartic nonlinearities is considered analytically based on an extended quasidiscreteness approach. For various mass differences (and thus different gap widths of the phonon spectrum), the coupled gap solitons are shown to display very rich dynamical behavior and their properties are strongly dependent on the force-constant ratio $K_3^2/(K_2K_4)$, where K_j $(j=1,2,3)$ are the force constants for the quadratic, cubic, and quartic parts of the intersite interaction potential, respectively. Several previous theoretical approaches for studying gap soliton dynamics in diatomic lattices are recovered in our scheme, and the relations between these methods are elucidated in a systematic way.

PACS number(s): 63.20.Pw, 63.20.Ry

I. INTRODUCTION

Anharmonicity in lattices is responsible for many important phenomena, such as transfer of energy, thermal conductivity, structural phase transitions, and the associated soft mode and central peak phenomena, etc. The study of nonlinear lattice dynamics and related lattice solitons has been greatly influenced by the pioneering work of Fermi, Pasta, and Ulam [1]. Most of the early work in this area focused on monatomic lattices. In recent years, much attention has been paid to nonlinear dynamics in diatomic lattices. The particular interest in studying the band gap and related nonlinear excitations [2–14] has been greatly stimulated by the discovery of optical gap solitons in periodic dielectric materials [15]. For a diatomic lattice, the phonon spectrum consists of two branches (acoustic and optical), induced by mass or force-constant differences. Due to the interplay between discreteness and nonlinearity, types of nonlinear localized excitations that have no direct analog in continuum models are possible. In particular, gap solitons may appear with their vibration frequencies in the phonon band gap. Since gap solitons occur in perfect lattices with discrete translational symmetry, the terms ''anharmonic gap mode'' and ''intrinsic gap mode'' have been used also [4,12]. It is possible that gap solitons may be created experimentally in diatomic lattices. References [16–18] reported observation of gap solitons in damped and parametrically driven one-dimensional (1D) diatomic pendulum lattices.

The mechanism for the appearance of gap solitons in nonlinear diatomic lattices can be briefly explained. Assume that there is an excited lattice wave with its vibration frequency falling within the phonon band gap. In the linear limit, such a lattice wave is strongly reflected (Bragg reflection). Only exponentially growing and decaying solutions for lattice displacements are possible and, for a finite system, an exponentially decaying solution results, leading to very low transmissivity. The situation is changed when the amplitude of the lattice wave is high enough. In this circumstance the nonlinearity of the system begins to play its role. If the nonlinearity has an appropriate sign, the exponentially growing and decaying solutions to the left and right can be connected in the large-amplitude region to form a self-consistent nonlinear localized solution that is finite everywhere. Such a solution is just the lattice gap soliton mentioned above.

There exist three different analytical approaches for the gap soliton dynamics in nonlinear diatomic lattices. The first one was provided by Kivshar and Flytzanis [3]. The starting point is that, in the case of small mass difference (thus a narrower phonon band gap), because of nonlinearity there exists a strong coupling between the optical lower cutoff mode and the acoustical upper cutoff mode at the boundary of the Brillouin zone (BZ). Under the rotating-wave approximation, they derived coupled nonlinear envelope equations for the two cutoff modes for the diatomic lattice with nonlinear on-site potential. Some interesting coupled soliton solutions were obtained. Later, this approach was used to study the coupled gap solitons in a diatomic lattice with nonlinear intersite potentials [19–21]. Such coupled-mode theory is similar to the corresponding theory for optical gap solitons in shallow nonlinear gratings [22], valid only for a narrow band gap, and the coupled-mode equations obtained are essentially the same as the coupled-mode equations obtained in Ref. [22].

The second theory was given by Konotop [11] based on an envelope function approach. In his approach Konotop also considered the small-band-gap case. However, instead of the coupled envelope equations he obtained a nonlinear Schrödinger (NLS) equation. The solitons obtained can propagate with the group velocity of the carrier wave at wave vector $q=\pi/d$ of the corresponding monatomic lattice with the lattice constant $d_0=d/2$, where d is the lattice constant of the diatomic lattice [11]. The solitons obtained by this approach display tails (companion modes) at the rear of the solitonic pulses.

The third method is based on a quasidiscreteness approach (QDA) [5,13]. The amplitude equation derived in this approach is also a NLS equation but it is valid for the whole BZ of the phonon spectrum. Using the results from the QDA, one can obtain various types of nonlinear excitation for acoustic and optical modes. In particular, for the cutoff modes at the BZ boundary, we can get the acoustic upper and optical lower cutoff gap solitons. Explicit criteria for the existence of gap solitons in nonlinear diatomic lattices can be obtained [13]. However, the coupling between the two cutoff modes at $q=\pi/d$ has not been considered in this approach and a difficulty exists when the width of the band gap becomes small. The difficulty can be seen from the expressions for the gap soliton amplitudes, which are proportional to $1/(M-m)$, where m and M are the mass of light and heavy particles, respectively. Thus the results for the gap solitons obtained from the QDA developed before [5,13] are valid only for single-mode excitations and for the large-band-gap case.

In a recent paper, Jiménez and Konotop [14] considered gap solitons in diatomic lattices with quartic intersite nonlinearity for different band gap widths. Some interesting results are discussed, in particular, the appearance of companion modes when solitons are excited. However, questions still exist: what is the relation between the above-mentioned three different approaches for gap soliton dynamics in nonlinear diatomic lattices? Is it possible to construct a general scheme to derive all the envelope equations obtained previously? What kinds of effects will occur when cubic nonlinearity, which is a common characteristic of standard interatomic potentials, such as the Toda, Born-Mayer-Coulomb, Lennard-Jones, and Morse types [13], is introduced into the model? It is just these problems that will be addressed here.

The paper is organized as follows. In Sec. II, the model Hamiltonian with cubic and quartic nonlinearities is introduced and the asymptotic expansions for several different cases are provided based on the QDA. The relative orders of magnitude for different smallness parameters appearing in the system are especially emphasized in making the asymptotic expansions. In Sec. III, we present some exact coupled lattice gap soliton solutions. We show that the properties of these coupled gap solitons are strongly dependent on the mass and force-constant ratios of the system. Finally, Sec. V contains a discussion and summary of our results.

II. MODEL AND ASYMPTOTIC EXPANSION

A. The model and preliminaries for asymptotic expansion

The model under investigation is a 1D diatomic lattice with a two-body nearest-neighbor interaction potential. The Hamiltonian of the system is given by

$$H=\sum_i\left[\frac{1}{2}m_i\left(\frac{du_i}{dt}\right)^2+V(u_{i+1}-u_i)\right],\qquad(1)$$

where $u_i=u_i(t)$ is the displacement from its equilibrium position of the ith particle with the mass $m_i=m\delta_{i,2k}+M\delta_{i,2k+1}$ ($M>m$, k is an integer). The potential $V(r)$ is quite general; typically it can be a standard two-body potential of Toda, Born-Mayer-Coulomb, Lennard-Jones, or Morse type (for their detailed expressions, see Ref. [14]). We focus on displacements with smaller amplitude; thus we Taylor expand the potential $V(r)$ at the equilibrium position $r=0$ in a power series of the displacements to fourth order. As a result we have an approximate K_2-K_3-K_4 potential $V(r)=\frac{1}{2}K_2r^2+\frac{1}{3}K_3r^3+\frac{1}{4}K_4r^4$, where K_2 (>0), K_3, and $K_4(>0)$ are harmonic, cubic, and quartic force constants, respectively. Obviously, $K_3=0$ if the potential $V(r)$ is symmetric. We assume that K_j ($j=2,3,4$) are of order unity. The equations of motion for the lattice displacements v_n (for light particles) and w_n (for heavy particles) are

$$m\frac{d^2}{dt^2}v_n=K_2(w_n+w_{n-1}-2v_n)+K_3[(w_n-v_n)^2-(w_{n-1}-v_n)^2]+K_4[(w_n-v_n)^3+(w_{n-1}-v_n)^3],\qquad(2)$$

$$M\frac{d^2}{dt^2}w_n=K_2(v_n+v_{n+1}-2w_n)-K_3[(v_n-w_n)^2-(v_{n+1}-w_n)^2]+K_4[(v_n-w_n)^3+(v_{n+1}-w_n)^3],\qquad(3)$$

where n is the index of the nth unit cell with the lattice constant $d=2d_0$, and d_0 is the equilibrium distance between two adjacent particles. The linear dispersion relation of the system is given by

$$\omega_\pm^2(q)=I_2+J_2\pm[(I_2+J_2)^2-4I_2J_2\sin^2(qd/2)]^{1/2},\qquad(4)$$

where $I_2=K_2/m$ and $J_2=K_2/M$. The minus (plus) sign corresponds to the acoustic (optical) mode. At wave number $q=0$ the eigenfrequency spectrum has a lower cutoff $\omega_-(0)=0$ for the acoustic phonon band and an upper cutoff $\omega_+(0)\equiv\omega_3=[2(I_2+J_2)]^{1/2}$ for the optical band. At $q=\pi/d$ there exists a band gap between the upper cutoff of the acoustic branch, $\omega_-(\pi/d)\equiv\omega_1=\sqrt{2J_2}$, and the lower cutoff of the optical branch, $\omega_+(\pi/a)\equiv\omega_2=\sqrt{2I_2}$. The width of the band gap is $\omega_2-\omega_1=\sqrt{2K_2}(1/\sqrt{m}-1/\sqrt{M})$, propotional to the mass difference $M-m$.

Because in general it is not possible to solve analytically nonlinear lattice equations of motion like Eqs. (2) and (3), some approximate theories have been developed. One powerful and clear-cut method is the method of multiple scales, a kind of singular perturbation theory widely used in the study of nonlinear waves, solitons, and pattern formation in continuous media [23,24]. In 1972, Tsurui [25] proposed the QDA for studying soliton excitations in nonlinear monatomic lattices. Later, the QDA was extended by several authors to nonlinear diatomic lattices [5,13,14]. The basic spirit of the QDA is the assumption that a linear plane lattice wave is weakly modulated by the nonlinearity of the system. The modulated wave consists of two parts. One is the carrier wave, which is taken to be completely discrete and a function of the ''fast'' variables n and t. The other one is an envelope (or amplitude), which is a function of the slow variables like $\xi_n=\epsilon(nd-\lambda t)$ and $\tau=\epsilon^2t$. Here λ is a constant given by a solvability condition. ϵ is a small and ordering parameter denoting the amplitude of the excitation. The envelope is determined by an ''envelope equation'' which is provided by another solvability condition. The solvability conditions here mean the conditions of eliminating secular terms in the asymptotic expansion. If several modes are considered simultaneously, a set of coupled-mode equations will result.

One important fact that should be stressed is that there are generally several small physical parameters appearing in the system. The small parameters can also be provided by the initial conditions for the excitation under consideration. The *relative orders of magnitude of these small parameters are of crucial importance for making an asymptotic expansion*. Different relations for these small parameters result in different envelope equations, which are valid only for different types of nonlinear excitation. We shall show in what follows that this is the key reason why there exist many different theoretical approaches for the gap soliton dynamics in diatomic lattices in the published literature.

In general, one can make the following assumptions for a nonlinear excitation in the system (2) and (3).

(1) The nonlinearity is weak, i.e.,

$$u_n(t)=\delta_1 u_n^{(1)}(t)+\delta_1^2 u_n^{(2)}(t)+\delta_1^3 u_n^{(3)}(t)+\cdots, \tag{5}$$

where δ_1 is a smallness parameter characterizing the *weakness* of the excitation. $u_n(t)$ represents either $v_n(t)$ or $w_n(t)$.

(2) The excitation is a quasiplane lattice wave, i.e., it is a plane lattice wave modulated in time and in space as

$$u_n^{(j)}(t)=u^{(j)}(\tau,\xi_n;\phi_n(t)) \tag{6}$$

$(j=1,2,3,\ldots)$ with

$$\tau=\delta_2 t, \tag{7}$$

$$\xi_n=\delta_3(nd-\lambda t), \tag{8}$$

$$\phi_n(t)=qnd-\omega(q)t, \tag{9}$$

where δ_2 and δ_3 are two smallness parameters accounting for the *slow variation* of the envelope of the excitation in space and time. $\phi_n(t)=qnd-\omega(q)t$ is the phase of the carrier wave, which is taken to be completely discrete in the QDA.

(3) The mass difference $M-m$ may be small, i.e.

$$m=\overline{m}-\delta m=\overline{m}(1-\delta_4\Delta), \tag{10}$$

$$M=\overline{m}+\delta m=\overline{m}(1+\delta_4\Delta), \tag{11}$$

where δ_4 represents the mass difference by $\delta_4=(M-m)/(2\overline{m})$ with $\overline{m}=(m+M)/2$ (the mean value). Δ is a constant with order unity. Clearly, δ_4 is a parameter manifesting the band *gap width* of the phonon spectrum.

For given values of m and M and given initial exciting conditions for the excitation in the system (2) and (3), the relative orders of magnitude of the parameters δ_j $(j=1,2,3,4)$ in Eqs. (5)–(11) should also be given. In fact, the property of the excitation is characterized by the relative orders of magnitude of these parameters. Without loss of generality, we can take $\delta_1=\epsilon$. Thus δ_j $(j=2,3,4)$ should be functions of ϵ, i.e., $\delta_j=\delta_j(\epsilon)$. In general, one can make the power-law assumption [23]

$$\delta_2=\epsilon^{\alpha},\quad \delta_3=\epsilon^{\beta},\quad \delta_4=\epsilon^{\gamma}. \tag{12}$$

Since we are interested in the nonlinear excitations that are formed by some kind of mechanism, e.g., the *balance* between the self-phase modulation and the dispersion of the system, the choice of α, β, and γ is not arbitrary in an asymptotic expansion [23].

B. Coupled-mode equations for wide band gap

In this subsection, we derive the coupled-mode equations for system (2) and (3) when the band gap width is large enough that we have $\gamma=0$ and thus $\delta_4=1$. By choosing $\alpha=2$ and $\beta=1$ we have the following scaling assumption:

$$u_n(t)=\epsilon u_{n,n}^{(1)}+\epsilon^2 u_{n,n}^{(2)}+\epsilon^3 u_{n,n}^{(3)}+\cdots, \tag{13}$$

$$\tau=\epsilon^2 t,\quad \xi_n=\epsilon(nd-\lambda t), \tag{14}$$

where $u_{n,n}^{(j)}\equiv u^{(j)}(\tau,\xi_n;\phi_n(t))$ $(j=1,2,3,\ldots)$. Substituting Eqs. (13) and (14) into Eqs. (2) and (3) we obtain the equations satisfied by $v_{n,n}^{(j)}$ and $w_{n,n}^{(j)}$ $(j=1,2,3,\ldots)$:

$$\frac{\partial^2}{\partial t^2}v_{n,n}^{(j)}-I_2(w_{n,n}^{(j)}+w_{n,n-1}^{(j)}-2v_{n,n}^{(j)})=M_{n,n}^{(j)}, \tag{15}$$

$$\frac{\partial^2}{\partial t^2}w_{n,n}^{(j)}-J_2(v_{n,n}^{(j)}+v_{n,n+1}^{(j)}-2w_{n,n}^{(j)})=N_{n,n}^{(j)}. \tag{16}$$

The concrete expressions for $M_{n,n}^{(j)}$ and $N_{n,n}^{(j)}$ are the same as in Ref. [14] and thus need not be repeated here. Equations (15) and (16) are now inhomogeneous but linear equations which can be solved order by order.

In the leading order $(j=1)$, we have generally the solution

$$w_{n,n}^{(1)}=F_{10}(\tau,\xi_n)+[F_{11}(\tau,\xi_n)\exp[i\phi_n^-(t)]+\text{c. c.}, \tag{17}$$

$$v_{n,n}^{(1)}=F_{10}(\tau,\xi_n)+[G_{11}(\tau,\xi_n)\exp[i\phi_n^+(t)]+\text{c. c.}], \tag{18}$$

where $\phi_n^{\pm}(t)=qnd-\omega_{\pm}(q)t$. F_{10} is the ''static'' part (dc component) of the excitation (which generates a strain field in the system) resulting from the cubic nonlinearity of the interaction potential. F_{11} (G_{11}) is the envelope of the ac part of the excitation for the acoustic (optical) mode. In contrast to Ref. [13], we are interested here in the coupling between the acoustic upper cutoff and the optical lower cutoff modes. Thus we set $q=\pi/d$. The leading-order solution (17) and (18) now takes the form

$$w_{n,n}^{(1)}=F_{10}(\tau,\xi_n)+[F_{11}(\tau,\xi_n)(-1)^n\exp(-i\omega_1 t)+\text{c. c.}], \tag{19}$$

$$v_{n,n}^{(1)}=F_{10}(\tau,\xi_n)+[G_{11}(\tau,\xi_n)(-1)^n\exp(-i\omega_2 t)+\text{c. c.}]. \tag{20}$$

For the second order $(j=2)$, the solvability condition of Eqs. (15) and (16) needs $\lambda=0$ thus $\xi_n=\epsilon nd$. The solution in this order reads

$$w_{n,n}^{(2)}=F_{20}+\Bigg(F_{21}(-1)^n\exp(-i\omega_1 t)-\frac{2J_3}{\omega_1\omega_2}F_{11}G_{11}\times\exp[-i(\omega_1+\omega_2)t]+\frac{2J_3}{\omega_1\omega_2}F_{11}^{*}G_{11}\times\exp[-i(\omega_2-\omega_1)t]+\text{c. c.}\Bigg),\qquad(21)$$

$$v_{n,n}^{(2)}=G_{20}+F_{20}-\frac{d}{2}\frac{\partial F_{10}}{\partial\xi_n}+\Bigg[\Bigg(G_{21}+\frac{I_2 d}{\omega_2^2-\omega_1^2}\frac{\partial F_{11}}{\partial\xi_n}\Bigg)(-1)^n\times\exp(-i\omega_1 t)+\frac{2I_3}{\omega_1\omega_2}F_{11}G_{11}\exp[-i(\omega_1+\omega_2)t]-\frac{2I_3}{\omega_1\omega_2}F_{11}^{*}G_{11}\exp[-i(\omega_2-\omega_1)t]+\text{c. c.}\Bigg],\qquad(22)$$

where F_{20}, G_{20}, F_{21}, and G_{21} are functions of ξ_n and τ, yet to be determined. We see that the appearence of the dc, sum-, and difference-frequency components in Eqs. (17)–(22) is due to the cubic nonlinearity in the interaction potential $(K_3\neq 0)$. It should be stressed that, unlike in the solution ansatz used in the literature, the staggered factor $(-1)^n$ does *not* appear in these components.

In the next order $(j=3)$, the solvability conditions require F_{10}, F_{11}, and G_{11} to be governed by the following coupled-mode equations:

$$\frac{\partial^2 F_{10}}{\partial\xi_n^2}+\frac{4J_3}{J_2 d}\frac{\partial}{\partial\xi_n}(|F_{11}|^2+|G_{11}|^2)=0,\qquad(23)$$

$$i\frac{\partial F_{11}}{\partial\tau}-\frac{I_2J_2d^2}{2\omega_1(\omega_2^2-\omega_1^2)}\frac{\partial^2 F_{11}}{\partial\xi_n^2}-\frac{J_3 d}{\omega_1}F_{11}\frac{\partial F_{10}}{\partial\xi_n}-\frac{3J_4}{\omega_1}(|F_{11}|^2+2|G_{11}|^2)F_{11}=0,\qquad(24)$$

$$i\frac{\partial G_{11}}{\partial\tau}+\frac{I_2J_2d^2}{2\omega_2(\omega_2^2-\omega_1^2)}\frac{\partial^2 G_{11}}{\partial\xi_n^2}-\frac{I_3 d}{\omega_2}G_{11}\frac{\partial F_{10}}{\partial\xi_n}-\frac{3I_4}{\omega_2}(|G_{11}|^2+2|F_{11}|^2)G_{11}=0.\qquad(25)$$

Equations (23)–(25) are coupled NLS systems with coupling to a mean term (dc field F_{10}). As in Ref. [26] we denote such equations as CNLSM. The case for excitation with a single cutoff mode (i.e., without any coupling between F_{11} and G_{11}) has been discussed in Refs. [5] and [13] in the absence and presence of cubic nonlinearity, respectively. We see that for the wide gap case the coupled interaction occurs between two cutoff modes through cross-phase modulations. The coupled gap soliton solutions of the CNLSM equations (23)–(25) will be given in Sec. III.

C. Coupled-mode equations for small band gap (I)

Now we derive the coupled-mode equations for a small band gap. In this case the cutoff modes at the BZ boundary have stronger coupling than in the wide-gap case. As in Ref. [14] by a small band gap we mean that γ, the parameter characterizing the width of the band gap, is equal to 2. Noting that for different excitations α and β in Eq. (12) may take different values, we have two interesting cases, which will be discussed in this and the next subsection.

The first case is for an excitation with relatively large extent (determined by the initial exciting condition), which is denoted by taking $\alpha=2$ and $\beta=2$. Thus one has

$$m=\bar{m}(1-\epsilon^2\Delta),\quad M=\bar{m}(1+\epsilon^2\Delta),\qquad(26)$$

$$\tau=\epsilon^2 t,\quad \xi_n=\epsilon^2(nd-\lambda t).\qquad(27)$$

It is obvious that λ can be taken to be zero because we have already introduced a slow-time-scale variable $\tau=\epsilon^2 t$. Thus we take $\lambda=0$ in the following calculation.

Substituting Eqs. (26), (27), and (13) into Eqs. (2) and (3), we obtain

$$\bar{m}\frac{\partial^2}{\partial t^2}v_{n,n}^{(j)}-K_2(w_{n,n}^{(j)}+w_{n,n-1}^{(j)}-2v_{n,n}^{(j)})=P_{n,n}^{(j)},\qquad(28)$$

$$\bar{m}\frac{\partial^2}{\partial t^2}w_{n,n}^{(j)}-K_2(v_{n,n}^{(j)}+v_{n,n+1}^{(j)}-2w_{n,n}^{(j)})=Q_{n,n}^{(j)}.\qquad(29)$$

The concrete expressions for $P_{n,n}^{(j)}$ and $Q_{n,n}^{(j)}$ for $j=1,2,3,\ldots$ are given in Appendix A.

At the leading order $(j=1)$, Eqs. (28) and (29) yield the solution

$$w_{n,n}^{(1)}=F_{10}+[F_{11}\exp(\phi_n)+\text{c. c.}],\qquad(30)$$

$$v_{n,n}^{(1)}=F_{10}+[G_{11}\exp(\phi_n)+\text{c. c.}],\qquad(31)$$

where F_{10}, F_{11}, and G_{11} are functions of τ and ξ_n $(=\epsilon^2 nd)$ and are yet to be determined. $\phi_n=qnd-\omega(q)t$ is the phase of the carrier wave with

$$\omega(q)=\left\{\frac{2K_2}{\bar{m}}\left[1-\cos\left(\frac{qd}{2}\right)\right]\right\}^{1/2}.\qquad(32)$$

It is obvious that Eq. (32) is the linear dispersion relation of a monatomic lattice with lattice constant $d_0=d/2$ and particle mass $\bar{m}$. Thus, in the leading order, the dynamics of the system is similar to that of a monatomic lattice. Shown in Fig. 1 are the dispersion curves $\omega_\pm(q)$ [see Eq. (4)] for the diatomic lattice and the dispersion curve $\omega(q)$ [i.e., Eq. (32)] for the monatomic lattice with mass $\bar{m}$. When $m\to M$ the band gap of the diatomic lattice at $q=\pi/d$ approaches zero and thus goes to the limit of the monatomic lattice.

Again we are interested in the cutoff modes at the BZ boundary (i.e., $q=\pi/d$). Then the solution (30) and (31) becomes

$$w_{n,n}^{(1)}=F_{10}+[F_{11}(-1)^n\exp(-i\bar{\omega}t)+\text{c. c.}],\qquad(33)$$

$$v_{n,n}^{(1)}=F_{10}+[G_{11}(-1)^n\exp(-i\bar{\omega}t)+\text{c. c.}],\qquad(34)$$

where $\bar{\omega}=\omega(q)|_{q=\pi/d}=[2K_2/\bar{m}]^{1/2}$ is the oscillating frequency of the carrier wave for the monatomic lattice with mass $\bar{m}$.

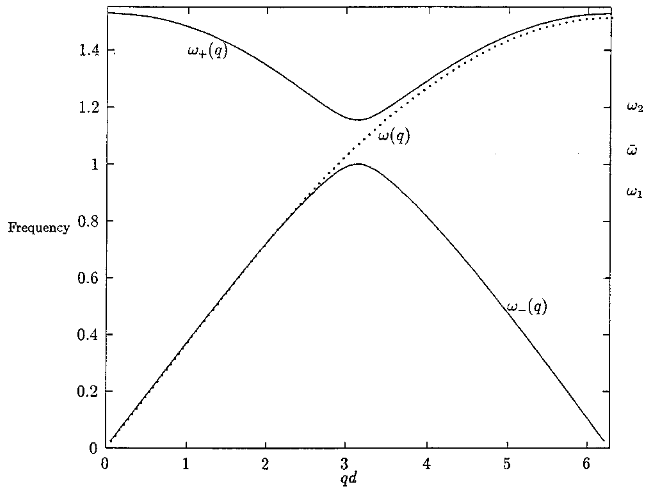

FIG. 1. The linear dispersion curves $\omega_\pm(q)$ for the diatomic lattice, given in Eq. (4). The phonon band gap appears at $qd=\pi$ with the gap width $\omega_2-\omega_1$ proportional to the mass difference $M-m$. The linear dispersion relation for the monatomic lattice with mass $\overline{m}$ is also shown as the dashed line. The gap vanishes for the diatomic lattice when $m\to M$; thus the system becomes continuously the monatomic lattice with mass m. The mass ratio $r_m=m/M=0.75$ and the frequency unit ω_1 are chosen for this figure.

At the next order $(j=2)$, the solution of Eqs. (28) and (29) reads

$$w_{n,n}^{(2)}=F_{20}+\bigg(F_{21}(-1)^n\exp(-i\overline{\omega}t)+\frac{K_3}{K_2}F_{11}G_{11}\exp(-2i\overline{\omega}t)+\text{c. c.}\bigg), \tag{35}$$

$$v_{n,n}^{(2)}=G_{20}+\bigg(G_{21}(-1)^n\exp(-i\overline{\omega}t)-\frac{K_3}{K_2}F_{11}G_{11}\exp(-2i\overline{\omega}t)+\text{c. c.}\bigg), \tag{36}$$

where F_{20}, G_{20}, and G_{21} are functions of τ and ξ_n, left undetermined at this level. In this order the dc terms F_{20} and G_{20} satisfy the relation

$$F_{20}-G_{20}=\frac{2K_3}{K_2}(F_{11}G_{11}^*+F_{11}^*G_{11}). \tag{37}$$

At the third order $(j=3)$, the solvability conditions of Eqs. (28) and (29) yield the following closed equations for F_{11} and G_{11}:

$$2i\overline{m\omega}\frac{\partial F_{11}}{\partial\tau}-K_2d\frac{\partial G_{11}}{\partial\xi_n}+\overline{m\omega}^2\Delta F_{11}-6K_4(|F_{11}|^2+2|G_{11}|^2)F_{11}+8K_4\bigg(\frac{K_3^2}{K_2K_4}-\frac{3}{4}\bigg)F_{11}^*G_{11}^2=0, \tag{38}$$

$$2i\overline{m\omega}\frac{\partial G_{11}}{\partial\tau}+K_2d\frac{\partial F_{11}}{\partial\xi_n}-\overline{m\omega}^2\Delta G_{11}-6K_4(|G_{11}|^2+2|F_{11}|^2)G_{11}+8K_4\bigg(\frac{K_3^2}{K_2K_4}-\frac{3}{4}\bigg)G_{11}^*F_{11}^2=0. \tag{39}$$

In contrast to the wide-band-gap case, here we see that there is no coupling between the dc component F_{10} and the ac components F_{11} and G_{11}. In contrast to the gap solitons in nonresonant quadratic optical media [27], here there is no couplings between F_{20} (and thus G_{20}) and F_{11}, G_{11}. In order to get the equation for F_{10} one must go to the fifth order $(j=5)$ of Eqs. (27) and (28). A straightforward calculation gives

$$\frac{\partial^2F_{10}}{\partial\tau^2}-v_1^2\frac{\partial^2F_{10}}{\partial\xi_n^2}=0, \tag{40}$$

where $v_1=[K_2d^2/(4\overline{m})]^{1/2}$ is the phase velocity at $q=0$ of the carrier wave for the monatomic lattice with mass $\overline{m}$.

Using the transformation [28] $F_\pm=(F_{11}\pm iG_{11})/2$, Eqs. (38) and (39) become

$$i\bigg(\frac{\partial}{\partial\tau}-v_2\frac{\partial}{\partial\xi_n}\bigg)F_-+\frac{1}{2}\overline{\omega}\Delta F_+-\frac{4K_4}{\overline{m\omega}}\bigg(\frac{3}{2}+\frac{K_3^2}{K_2K_4}\bigg)|F_-|^2F_-+\frac{4K_4}{\overline{m\omega}}\bigg(\frac{3}{2}-\frac{K_3^2}{K_2K_4}\bigg)F_+^2F_-^*-\frac{8K_4}{\overline{m\omega}}\bigg(\frac{3}{2}-\frac{K_3^2}{K_2K_4}\bigg)\times|F_+|^2F_-=0, \tag{41}$$

$$i\bigg(\frac{\partial}{\partial\tau}+v_2\frac{\partial}{\partial\xi_n}\bigg)F_++\frac{1}{2}\overline{\omega}\Delta F_--\frac{4K_4}{\overline{m\omega}}\bigg(\frac{3}{2}+\frac{K_3^2}{K_2K_4}\bigg)|F_+|^2F_++\frac{4K_4}{\overline{m\omega}}\bigg(\frac{3}{2}-\frac{K_3^2}{K_2K_4}\bigg)F_-^2F_+^*-\frac{8K_4}{\overline{m\omega}}\bigg(\frac{3}{2}-\frac{K_3^2}{K_2K_4}\bigg)\times|F_-|^2F_+=0, \tag{42}$$

where $v_2=K_2d/(2\overline{m\omega})$ is the group velocity at $q=\pi/d$ of the carrier wave of the monatomic lattice with mass $\overline{m}$. Equations (41) and (42) are a generalized version of the coupled-mode equations. Such coupled-mode equations were first derived for describing the coupled gap solitons in nonlinear periodic optical media with a shallow grating [22]. Later, a generalization to a deep grating was made by de Sterke *et al.* [29]. For convienence we hereafter call Eqs. (38) and (39) or (41) and (42) the generalized coupled-mode equations.

We note that, in the context of nonlinear lattice dynamics, the coupled-mode equations were first derived for an on-site interaction potential using the rotating-wave approximation (i.e., without any companion mode considered) [3] or by a special ansatz for solution in perturbation expansions [20]. In our derivation based on the QDA provided above, such an approximation or ansatz is not necessary and the procedure for the derivation is clear-cut from the viewpoint of singular perturbation theory [23].

D. Coupled-mode equations for small band gap (II)

The second case for small band gap ($\gamma=2$) is the situation where the extent of the excitation is not very large, i.e., we have $\alpha=2$ and $\beta=1$. Hence one has

$$m=\overline{m}(1-\epsilon^2\Delta),\quad M=\overline{m}(1+\epsilon^2\Delta),$$

$$\tau=\epsilon^2 t,\quad \xi_n=\epsilon(nd-\lambda t). \tag{43}$$

By substituting Eqs. (43) and (13) into Eqs. (2) and (3) one obtains

$$\overline{m}\frac{\partial^2}{\partial t^2}v_{n,n}^{(j)}-K_2(w_{n,n}^{(j)}+w_{n,n-1}^{(j)}-2v_{n,n}^{(j)})=R_{n,n}^{(j)}, \tag{44}$$

$$\overline{m}\frac{\partial^2}{\partial t^2}w_{n,n}^{(j)}-K_2(v_{n,n}^{(j)}+v_{n,n+1}^{(j)}-2w_{n,n}^{(j)})=S_{n,n}^{(j)}. \tag{45}$$

We see that the expressions on the left hand side of Eqs. (44) and (45) are the same as those in Eqs. (28) and (29) but the corresponding right hand side is now different. Detailed formulations for $R_{n,n}^{(j)}$ and $S_{n,n}^{(j)}$ ($j=1,2,3,\ldots$) have been listed in Appendix B.

The leading-order solution ($j=1$) of Eqs. (44) and (45) is the same as that of Eqs. (28) and (29) because $R_{n,n}^{(1)}=S_{n,n}^{(1)}=0$. At the BZ boundary, the solution is expressed again by Eqs. (33) and (34) but one should note that F_{10}, F_{11}, and G_{11} are now yet to be determined functions of $\tau=\epsilon^2 t$ and $\xi_n=\epsilon(nd-\lambda t)$.

At the second order ($j=2$), the solvability condition yields $\lambda=s_1\lambda_0$ with $\lambda_0=v_2=(d\omega/dq)|_{q=\pi/d}=K_2 d/(2\overline{m\omega})$, and

$$G_{11}=-is_1F_{11}, \tag{46}$$

where $s_1=\pm1$. Thus in this case F_{11} and G_{11} are no longer independent of each other. The second-order solution reads

$$w_{n,n}^{(2)}=F_{20}+\left(F_{21}(-1)^n\exp(-i\overline{\omega}t)+is_1\frac{K_3}{K_2}F_{11}^2\right.$$
$$\left.\times\exp(-2i\overline{\omega}t)+\text{c. c.}\right), \tag{47}$$

$$v_{n,n}^{(2)}=G_{20}+\left(G_{21}(-1)^n\exp(-i\overline{\omega}t)-is_1\frac{K_3}{K_2}F_{11}^2\right.$$
$$\left.\times\exp(-2i\overline{\omega}t)+\text{c. c.}\right), \tag{48}$$

with F_{20}, G_{20}, and G_{21} left as undetermined functions. There exists a relation between the dc terms F_{20} and G_{20}:

$$F_{20}-G_{20}=\frac{d}{2}\frac{\partial F_{10}}{\partial\xi_n}. \tag{49}$$

At the third order ($j=3$), the solvability conditions of Eqs. (44) and (45) require

$$\frac{\partial^2F_{10}}{\partial\xi_n^2}+\frac{16K_3}{K_2d}\frac{\partial}{\partial\xi_n}(|F_{11}|^2)=0, \tag{50}$$

$$i\frac{\partial F_{11}}{\partial\tau}-\frac{K_2d^2}{16\overline{m\omega}}\frac{\partial^2F_{11}}{\partial\xi_n^2}-\frac{K_3d}{\overline{m\omega}}F_{11}\frac{\partial F_{10}}{\partial\xi_n}-\frac{4K_4}{\overline{m\omega}}$$
$$\times\left(\frac{K_3^2}{K_2K_4}+\frac{3}{2}\right)|F_{11}|^2F_{11}=0, \tag{51}$$

$$\frac{\partial F_{21}}{\partial\xi_n}-\frac{d}{4}\frac{\partial^2F_{11}}{\partial\xi_n^2}+is_1\frac{\Delta}{2d}F_{11}=0. \tag{52}$$

This set of equations was derived by Konotop and coworkers in the absence of cubic nonlinearity [11,14]. If $K_3=0$, we have $F_{10}=0$. The dc terms (F_{20} and G_{20}) and the second harmonic terms in Eqs. (47) and (48) also disappear. Thus the second-order solution (companion mode) includes only the fundamental harmonic wave proportional to the leading-order solution (principal mode). In contrast to the cases discussed in the last two subsections, F_{21} (and thus G_{21}) here is controlled by Eq. (52), i.e., F_{21} is determined by F_{11} through

$$F_{21}=\frac{d}{4}\frac{\partial F_{11}}{\partial\xi_n}-is_1\frac{\Delta}{2d}\int F_{11}d\xi_n. \tag{53}$$

Up to now we have derived coupled-mode equations for the dynamics of coupled gap solitons for the *wide* band gap ($\gamma=0$) and the *small* band gap ($\gamma=2$). The relation between three different gap soliton theories existing in the literature [3,19–21,11,14,5,13] is now clear. We see that, in the scheme provided here, these different theoretical approaches correspond to different gap widths and different spatial-temporal extents of the excitations, i.e., they refer to different values of α, β, and γ, as denoted by the relation (12). Furthermore, the inclusion of the cubic nonlinearity (i.e., $K_3\neq0$) gives rise to many additional features for coupled gap solitons, which will be described in Sec. III below.

Let us now discuss two other cases, $\gamma=1$ (intermediate band gap) and $\gamma\geqslant3$ (negligible band gap). For the case of the negligible band gap, δm [see Eqs. (10) and (11)] can be ignored to the fourth order in the perturbation expansion. Our results show that the envelope equations can be obtained in the third-order perturbation expansion and they are the same as Eqs. (50) and (51), which are the envelope equations for the monatomic lattice with mass $\overline{m}$, but the constraint between F_{21} and F_{11}, i.e., Eq. (52), is no longer imposed. Hence for negligible band gap the respective envelope solitons display all the dynamical features of the monatomic lattice with mass $\overline{m}$, as also discussed in Ref. [30].

The second case not discussed so far is for an intermediate band gap, i.e., $\gamma=1$. It seems that in this case one cannot arrive at any significant nonlinear coupled-mode envelope equations because the envelope equations

$$2i\overline{m\omega}\frac{\partial F_{11}}{\partial\tau}-K_2d\frac{\partial G_{11}}{\partial\xi_n}+\overline{m\omega^2}\Delta F_{11}=0, \tag{54}$$

$$2i\overline{m\omega}\frac{\partial G_{11}}{\partial\tau}+K_2d\frac{\partial F_{11}}{\partial\xi_n}-\overline{m\omega^2}\Delta G_{11}=0 \tag{55}$$

appear as the solvability conditions in the second order in the perturbation expansion. Equations (54) and (55) are linear, dispersive equations which can easily be solved. Under such circumstances a distortionless pulse propagation is impossible [14].

III. COUPLED GAP SOLITON SOLUTIONS

A. Coupled soliton solutions for wide band gap

In this subsection we consider the soliton solutions of the coupled-mode equations (23)–(25). Integrating Eq. (23) once with respect to ξ_n and using the transformation $u=\epsilon F_{10}$, $v=\epsilon G_{11}\exp[i(I_3d/\omega_2)C_0t]$, and $w=\epsilon F_{11}\exp[i(J_3d/\omega_1)C_0t]$, we obtain

$$i\frac{\partial w}{\partial t}-g_w\frac{\partial^2 w}{\partial x_n^2}+p_w(|w|^2+\sigma|v|^2)w=0, \tag{56}$$

$$i\frac{\partial v}{\partial t}+g_v\frac{\partial^2 v}{\partial x_n^2}+p_v(|v|^2+\sigma|w|^2)w=0, \tag{57}$$

$$\frac{\partial u}{\partial x_n}=-\frac{4K_3}{K_2d}(|v|^2+|w|^2)+C_0, \tag{58}$$

when returning to the original variables. Here $x_n=nd$ and C_0 is an integration constant. The coefficients in Eqs. (56)–(58) are defined by

$$g_w=\frac{K_2^2d^2}{4\omega_1(M-m)}, \tag{59}$$

$$g_v=\frac{K_2^2d^2}{4\omega_2(M-m)}, \tag{60}$$

$$p_w=2\omega_1\frac{K_4}{K_2}\left(\frac{K_3^2}{K_2K_4}-\frac{3}{4}\right), \tag{61}$$

$$p_v=2\omega_2\frac{K_4}{K_2}\left(\frac{K_3^2}{K_2K_4}-\frac{3}{4}\right), \tag{62}$$

$$\sigma=\frac{K_3^2/(K_2K_4)-3/2}{K_3^2/(K_2K_4)-3/4}. \tag{63}$$

Equations (56) and (57) are coupled nonlinear Schrödinger equations. Many authors have considered their coupled soliton solutions for some particular coefficients [31]. However, we note that Eqs. (56)–(58) have several interesting characteristics that should be stressed. The first is that the second-order derivative terms for v and w, with respect to x_n, have opposite signs. This is due to the fact that the acoustic upper cutoff and optical lower cutoff modes have opposite group velocity dispersions. Generally, the coupled soliton solutions in this situation are bright-dark (i.e., soliton-kink) type [31]. As we shall show below, this conclusion is no longer valid when the cubic nonlinearity is taken into account (i.e., when $K_3\neq0$). The second feature is that the terms representing the cross-phase modulation (i.e., the terms $|v|^2w$ and $|w|^2v$) vanish if the force-constant ratio $r_k\equiv K_3^2/(K_2K_4)$, is equal to 3/2, which is just the case for the Toda and Morse potentials [13]. In this circumstance the motions of the two cutoff modes are independent of each other, although the nonlinearity in the system still play its role through the self-phase modulation, denoted by the terms $|v|^2v$ and $|w|^2w$. Furthermore, when $r_k=3/4$, the self-phase modulation disappears and thus the two cutoff modes interact through the cross-phase modulation. Depending on the mass ratio $r_m\equiv m/M$ and the force-constant ratio r_k defined above, the coupled soliton solutions can be divided into three different categories, which are listed below.

(a) *Soliton-soliton excitations*. If r_m and r_k satisfy the condition

$$f_1(r_m)<r_k<\frac{9}{8}, \tag{64}$$

where the function f_1 is defined by

$$f_1(x)=\frac{3(1+2x)}{4(1+x)}, \tag{65}$$

Equations (56)–(58) admit the coupled soliton-soliton solution

$$w=W_0\,\mathrm{sech}(kx_n+2g_wkk_1t)\exp[i(k_1x_n-\Omega_1t)], \tag{66}$$

$$v=V_0\,\mathrm{sech}(kx_n-2g_vkk_2t)\exp[i(k_2x_n-\Omega_2t)], \tag{67}$$

$$u=-\frac{4K_3}{K_2d}k(V_0^2+W_0^2)\tanh(kx_n+2g_wkk_1t)+C_0x_n, \tag{68}$$

with

$$W_0^2=\frac{2k^2}{\sigma^2-1}\left(\frac{g_w}{p_w}+\sigma\frac{g_v}{p_v}\right), \tag{69}$$

$$V_0^2=\frac{2k^2}{1-\sigma^2}\left(\frac{g_v}{p_v}+\sigma\frac{g_w}{p_w}\right), \tag{70}$$

$$\Omega_1=g_w(k^2-k_1^2), \tag{71}$$

$$\Omega_2=g_v(k_2^2-k^2), \tag{72}$$

where $k_2=-(g_w/g_v)k_1$ and k,k_1 are two free parameters. In order that the energy of the excitation be finite, one should take the integration constant $C_0=0$. The lattice configuration in this case takes the form

$$w_n(t) = -\frac{4K_3}{K_2 d}k(V_0^2+W_0^2)\tanh(knd+2g_w kk_1 t) + (-1)^n 2W_0 \,\mathrm{sech}(knd+2g_w kk_1 t) \times\cos[k_1 nd-(\omega_1+\Omega_1)t], \quad (73)$$

$$v_n(t) = -\frac{4K_3}{K_2 d}k(V_0^2+W_0^2)\tanh(knd-2g_v kk_2 t) + (-1)^n 2V_0 \,\mathrm{sech}(knd-2g_v kk_2 t) \times\cos[k_2 nd-(\omega_2+\Omega_2)t]. \quad (74)$$

Thus the displacements of both light and heavy particles have an ac component plus a dc background (mean field). If k_1 (and thus k_2) vanishes, the excitation described by Eqs. (73) and (74) is an asymmetric standing soliton-soliton pair in which the oscillating frequency of the acoustic upper cutoff mode is increased but that of the optical lower cutoff mode is lowered. Thus both of the oscillating frequencies are within the band gap of the phonon spectrum. Accordingly, if the Hamiltonian of a system has a cubic nonlinearity, it is hard to say the nonlinearity of the system is ''hard'' or ''soft.''

(b). *Kink-soliton excitations*. In the case that r_m and r_k obey the relation

$$r_k < f_1(r_m) \quad \text{or} \quad r_k > f_2(r_m), \quad (75)$$

where the function f_2 is defined by

$$f_2(x) = \frac{3(2+x)}{4(1+x)}, \quad (76)$$

Equations (56)–(58) have the coupled kink-soliton solution

$$w = W_0 \tanh(kx_n+2g_w kk_1)\exp[i(k_1 x_n - \Omega_1 t)], \quad (77)$$

$$v = V_0 \,\mathrm{sech}(kx_n-2g_v kk_2 t)\exp[i(k_2 x_n - \Omega_2 t)], \quad (78)$$

$$u = -\frac{4K_3}{K_2 d}k(V_0^2-W_0^2)\tanh(kx_n+2g_w kk_1 t), \quad (79)$$

with

$$W_0^2 = \frac{2k^2}{1-\sigma^2}\left(\frac{g_w}{p_w}+\sigma\frac{g_v}{p_v}\right), \quad (80)$$

$$V_0^2 = \frac{2k^2}{1-\sigma^2}\left(\frac{g_v}{p_v}+\sigma\frac{g_w}{p_w}\right), \quad (81)$$

$$\Omega_1 = -g_w(2k^2-k_1^2)-\sigma p_w V_0^2, \quad (82)$$

$$\Omega_2 = g_v(k_2^2-k^2)-\sigma p_v W_0^2, \quad (83)$$

where $k_2 = -(g_w/g_v)k_1$ and k,k_1 are still two free parameters. In order to make the excitation energy finite, we have taken $C_0 = 4K_3 W_0^2/(K_2 d)$. The lattice displacement in this case reads as

$$w_n(t) = -\frac{4K_3}{K_2 d}k(V_0^2-W_0^2)\tanh(knd+2g_w kk_1 t) + (-1)^n 2W_0 \tanh(knd+2g_w kk_1 t) \times\cos[k_1 nd-(\omega_1+\Omega_1-\beta_1 C_0)t], \quad (84)$$

$$v_n(t) = -\frac{4K_3}{K_2 d}k(V_0^2-W_0^2)\tanh(knd-2g_v kk_2 t) + (-1)^n 2V_0 \,\mathrm{sech}(knd-2g_v kk_2 t) \times\cos[k_2 nd-(\omega_2+\Omega_2-\beta_2 C_0)t], \quad (85)$$

with $\beta_1 = -K_3 d/(M\omega_1)$ and $\beta_2 = -K_3 d/(m\omega_2)$. If k_1 (and thus k_2) vanishes, Eqs. (84) and (85) represent a standing kink-soliton pair. Depending on r_m and r_k, the oscillating frequency of the ac component for both $w_n(t)$ and $v_n(t)$ may be inside or outside the band gap.

(c). *Kink-kink excitations*. If r_m and r_k satisfy the relation

$$\frac{9}{8} < r_k < f_2(r_m), \quad (86)$$

Equations (56)–(58) yield the coupled kink-kink solution

$$w = W_0 \tanh(kx_n+2g_w kk_1)\exp[i(k_1 x_n - \Omega_1 t)], \quad (87)$$

$$v = V_0 \tanh(kx_n-2g_v kk_2 t)\exp[i(k_2 x_n - \Omega_2 t)], \quad (88)$$

$$u = -\frac{4K_3}{K_2 d}k(V_0^2+W_0^2)\tanh(kx_n+2g_w kk_1 t), \quad (89)$$

with

$$W_0^2 = \frac{2k^2}{1-\sigma^2}\left(\frac{g_w}{p_w}+\sigma\frac{g_v}{p_v}\right), \quad (90)$$

$$V_0^2 = \frac{2k^2}{1-\sigma^2}\left(\frac{g_v}{p_v}+\sigma\frac{g_w}{p_w}\right), \quad (91)$$

$$\Omega_1 = -g_w(2k^2+k_1^2), \quad (92)$$

$$\Omega_2 = g_v(2k^2+k_2^2), \quad (93)$$

where $k_2 = -(g_w/g_v)k_1$ and k,k_1 are again free parameters. The requirement of the excitation energy to be finite needs $C_0 = 4K_3(V_0^2+W_0^2)/(K_2 d)$. The corresponding lattice configuration for this case can also be written down but we omitted it here.

It should be stressed that the soliton-kink excitation (i.e., the ac component for the acoustic upper cutoff mode is a soliton while the ac component for the optical lower cutoff mode is a kink) does not exist in our system (2) and (3). In Fig. 2 we have shown the different existence regions for all possible coupled soliton excitations in the parameter space of r_m and r_k. We see that r_m and r_k *are two important parameters for controlling what coupled solitons occur*. For a symmetric potential, $r_k = 0$, only one type of coupled soliton, i.e., the kink-soliton, is allowed. However, note that the standard interatomic potentials, i.e., the Toda, Born-Mayer-Coulomb, Lennard-Jones, and Morse potentials, have a cubic nonlin-

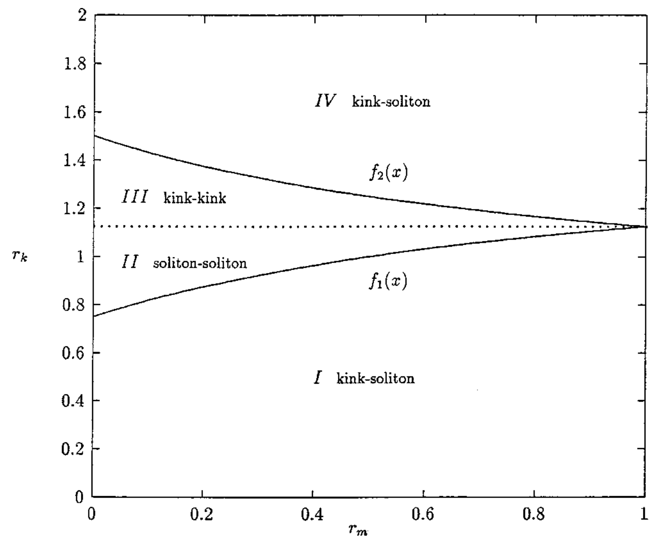

FIG. 2. Overview of different existence regions for coupled gap soliton excitations in the case of a wide band gap. In the regions I and IV coupled kink-solitons exist; while in II and III the system displays soliton-soliton and kink-kink excitations, respectively.

earity and hence $r_k \neq 0$ [13]. Consequently, realistic lattice systems display more types of coupled gap solitons than those obtained from a simple model based on symmetric potentials.

The single-mode excitations (i.e., $F_{11} \neq 0$, $G_{11}=0$ or $F_{11}=0$, $G_{11} \neq 0$) for Eqs. (23)–(25) have been studied before [13]. Here we note that the type of each single-mode excitation can be changed when the coupling between two cutoff modes is taken into account. The physical reason for this change is the cross-phase modulation, as pointed out recently in Ref. [32].

B. Coupled soliton solutions for small band gap (I)

Let us now discuss the coupled soliton solutions of the coupled-mode equations (38) and (39). To use the original variables we set $f=\epsilon F_{11}$ and $g=\epsilon G_{11}$. Then we have

$$2\overline{m\omega}\left(i\frac{\partial}{\partial t}+\Omega_0\right)f-K_2 d\frac{\partial g}{\partial x_n}-6K_4(|f|^2+2|g|^2)f +8K_4\left(r_k-\frac{3}{4}\right)f^* g^2=0, \tag{94}$$

$$2\overline{m\omega}\left(i\frac{\partial}{\partial t}-\Omega_0\right)g+K_2 d\frac{\partial f}{\partial x_n}-6K_4(|g|^2+2|f|^2)g +8K_4\left(r_k-\frac{3}{4}\right)g^* f^2=0, \tag{95}$$

with $x_n=nd$ and $\Omega_0=\epsilon^2\overline{\omega}/2$. For convenience we have set $\Delta=1$ and hence $\epsilon^2=(M-m)/(M+m)=(1-r_m)/(1+r_m)$. A generalized version of Eqs. (94) and (95) was obtained by de Sterke *et al.* in the context of nonlinear optics [29].

We seek stationary soliton solutions of Eqs. (94) and (95) by use of the method developed by Kivshar and Flytzanis [3]. Thus we set

$$f(x_n,t)=f(x_n)\exp(-i\Omega t), \tag{96}$$

$$g(x_n,t)=g(x_n)\exp(-i\Omega t), \tag{97}$$

where Ω is a frequency detuning, and $f(x_n)$ and $g(x_n)$ are two real functions yet to be determined. Substitution of Eqs. (96) and (97) into Eqs. (94) and (95) results in

$$\frac{df}{dz}=-\gamma_2 g+g^3+\eta f^2 g, \tag{98}$$

$$\frac{dg}{dz}=\gamma_1 f-f^3-\eta f g^2, \tag{99}$$

with $z=[6K_4/(K_2 d)]x_n$, $\eta=4(9/4-r_k)/3$, $\gamma=[\overline{m\omega}/(3K_4)](\Omega+\Omega_0)$, and $\gamma_2=[\overline{m\omega}/(3k_4)](\Omega-\Omega_0)$. Equations (98) and (99) are similar to the equations obtained by Kivshar and Flytzanis [3], and their qualitative features were analyzed recently through the bifurcation picture without considering cubic nonlinearity [21]. In our system here the force-constant ratio r_k (or equivalent η) and the frequency detuning Ω are two important parameters for controlling the property of the soliton solutions, as shown below. Equations (98) and (99) form a Hamiltonian system in which g and f play, respectively, the roles of p and q, and the Hamiltonian is

$$\mathcal{H}=\frac{1}{2}\gamma_1 f^2+\frac{1}{2}\gamma_2 g^2-\frac{1}{4}(f^2+g^2)-\frac{1}{2}\eta f^2 g^2. \tag{100}$$

By introducing the function $h(z)=g(z)/f(z)$, Eqs. (98) and (99) can be solved exactly through integration of the equation

$$\frac{dh}{dz}=-s_1[(\gamma_1+\gamma_2 h)^2-4E(1+2\eta h^2+h^4)]^{1/2}, \tag{101}$$

where $s_1=\pm 1$ and E is the value of the ''energy'' corresponding to the particular orbit associated with the Hamiltonian $\mathcal{H}$. The solutions for f and g may be found with the help of the relations

$$f^2=\frac{\gamma_1+\gamma_2 h^2 \pm[(\gamma_1+\gamma_2 h^2)^2-4E(1+2\eta h^2+h^4)]^{1/2}}{1+2\eta h^2+h^4}, \tag{102}$$

$$g=fh. \tag{103}$$

In the phase plane (f,g), the separatrixes correspond to soliton or kink solutions of different types. The phase portrait of the system depends on the parameters r_k and Ω. For a given r_k, as Ω increases a number of subsequent bifurcations in the plane take place. By analyzing the critical points on the phase plane, we can distinguish three different regimes.

(1) $\Omega<-\Omega_0$. In this regime both γ_1 and γ_2 are negative and the oscillating frequency of the lattice $(\overline{\omega}+\Omega)$ satisfies the condition

$$\overline{\omega}+\Omega<\left(\frac{2}{1+r_m}\right)^{1/2}\frac{1+3r_m}{2(1+r_m)}\omega_1. \tag{104}$$

We find that the origin (0,0) is the only fixed point and that it is a stable center. Thus there is no soliton solution.

(2) $-\Omega_0<\Omega<\Omega_0$. This is the case for $\gamma_1>0$ and $\gamma_2<0$, and hence

$$\left(\frac{2}{1+r_m}\right)^{1/2}\frac{1+3r_m}{2(1+r_m)}\omega_1<\bar{\omega}+\Omega<\left(\frac{2r_m}{1+r_m}\right)^{1/2}\frac{3+r_m}{2(1+r_m)}\omega_2. \tag{105}$$

In this situation the system (98) and (99) has a saddle at (0,0) and two centers at $(\pm\sqrt{\gamma_1},0)$. Independent of r_k, the only type of localized solution corresponds to the separatrix connecting (0,0) with itself (thus $E=0$), corresponding to a bright soliton. Solving Eqs. (101)–(103), we obtain

$$h=-(\gamma_1/|\gamma_2|)^{1/2}\tanh y, \tag{106}$$

$$f=s_1\frac{\sqrt{2\gamma_1}\operatorname{sech} y}{[1+2\eta(\gamma_1/|\gamma_2|)\tanh^2 y+(\gamma_1/|\gamma_2|)^2\tanh^4 y]^{1/2}}, \tag{107}$$

$$g=-s_1\gamma_1\sqrt{\frac{2}{|\gamma_2|}}\times\frac{\tanh y\operatorname{sech} y}{[1+2\eta(\gamma_1/|\gamma_2|)\tanh^2 y+(\gamma_1/|\gamma_2|)^2\tanh^4 y]^{1/2}}, \tag{108}$$

where $y=\sqrt{\gamma_1|\gamma_2|}(z-z_0)$ with z_0 an arbitrary constant. We see that in this case both envelopes of the vibrations for heavy and light particles are solitons. However, they are different kinds of solitons since the soliton f (for the heavy particles) is symmetric with only one maximum but the soliton g (for the light particles) is asymmetric and there are two extrema.

(3) $\Omega>\Omega_0$. In this regime both γ_1 and γ_2 are positive. The corresponding oscillating frequency is located in the region

$$\bar{\omega}+\Omega>\left(\frac{2r_m}{1+r_m}\right)^{1/2}\frac{3+r_m}{2(1+r_m)}\omega_2. \tag{109}$$

There exists now a larger number of critical points, the character of which depends on the relative sizes of the force-constant ratio r_k and the the detuning Ω. Four possible types of critical points for this regime are listed in Table I. The critical point at the origin (0,0) (type I) is always a center for all r_k and Ω $(>\Omega_0)$, and hence no soliton is possible. The nature of the other types of critical points depends on r_k and Ω. Details can be found in Table II. For each separatrix the shape of the soliton excitation may be found explicitly by integrating Eq. (101) using the corresponding value of the ''energy'' E. For example, in the case of $0<r_k<3/2$ and $\Omega>(1+\eta)\Omega_0/(\eta-1)$, the critical points $(0,\pm\sqrt{\gamma_2})$ and $(\pm\sqrt{\gamma_1},0)$ are centers while the critical points $(\pm[(\gamma_1-\eta\gamma_2)/(1-\eta^2)]^{1/2},\pm[(\gamma_2-\eta\gamma_1)/(1-\eta^2)])$ are saddles.

TABLE I. The positions of the critical points in the phase plane (f,g) for $\Omega>\Omega_0$. The definitions of the parameters γ_1,γ_2, and η have been given in the text.

Type	f	g
I	0	0
II	0	$\pm\sqrt{\gamma_2}$
III	$\pm\sqrt{\gamma_1}$	0
IV	$\pm\sqrt{\frac{\gamma_1-\eta\gamma_2}{1-\eta^2}}$	$\pm\sqrt{\frac{\gamma_2-\eta\gamma_1}{1-\eta^2}}$

Through the saddles we have $E=(\gamma_1^2+\gamma_2^2-2\eta\gamma_1\gamma_2)/[4(\eta^2-1)]$. Integrating Eq. (101) for this case we find that

$$h=s_2C_1\tanh y \tag{110}$$

with $s_2=\pm 1$, $C_1=(\gamma_1\eta-\gamma_2)/(\gamma_2\eta-\gamma_1)$, and $y=[(\gamma_1\eta-\gamma_2)/(\eta^2-1)]^{1/2}(z-z_0)$. Using Eqs. (102) and (103) we obtain

$$f=s_3\left(\frac{\gamma_1+\gamma_2C_1^2\tanh^2 y-s_2C_1C_2\operatorname{sech}^2 y}{1+2\eta C_1^2\tanh^2 y+C_1^4\tanh^4 y}\right)^{1/2}, \tag{111}$$

$$g=s_2s_3\tanh y\left(\frac{\gamma_1+\gamma_2C_1^2\tanh^2 y-s_2C_1C_2\operatorname{sech}^2 y}{1+2\eta C_1^2\tanh^2 y+C_1^4\tanh^4 y}\right)^{1/2}, \tag{112}$$

where $s_3=\pm 1$ and $C_2=[(\gamma_1\eta-\gamma_2)/(\eta^2-1)]^{1/2}$. Each of these solutions (for different s_j, $j=2,3$) is a kink connecting a saddle to another saddle.

We note that the three regimes discussed above correspond to the cases that the oscillating frequencies of the lattice are located below, within, and above the band gap of the phonon spectrum, respectively. For instance, when $\epsilon=0.1$ we have $r_m=0.98$. The regimes expressed in Eqs. (104), (105), and (109) are $\bar{\omega}+\Omega<0.99\omega_1$, $0.99\omega_1<\bar{\omega}+\Omega<1.01\omega_2$, and $\bar{\omega}+\Omega>1.01\omega_2$, respectively. If $r_m\to 1$, they correspond respectively to $\bar{\omega}+\Omega<\omega_1$, $\omega_1<\bar{\omega}+\Omega<\omega_2$, and $\bar{\omega}+\Omega>\omega_2$. Thus r_m is the parameter controlling the oscillating frequency of the system.

We know that all standard two-body interatomic potentials display cubic nonlinearity (i.e., $r_k\neq 0$); and for different potentials r_k takes different values [13]. The results presented above can be applied to two-body potentials from Lennard-Jones ($r_k=63/53$) and Toda and Morse ($r_k=3/2$) to Born-Mayer-Coulomb ($r_k=3I/2$, $I>1$; some typical values of I have been given in Ref. [13]). From Table II we see that there are different critical points for different two-body interaction potentials and hence different gap solitons. Thus the introduction of the cubic nonlinearity gives rise to many defferent types of coupled gap soliton excitations in the system.

TABLE II. Nature of the critical points and their existence conditions for the case $\Omega>\Omega_0$. $r_k=K_3^2/(K_2K_4)$ is the force-constant ratio of the system. The parameters η and Ω_0 have been given in the text. In the last column the standard two-body potentials [i.e., Lennard-Jones (L-J), Toda, Morse, Born-Mayer-Coulomb (B-M-C)] are listed in the corresponding regions of r_k.

Condition 1	Condition 2	Type II	Type III	Type IV	Application
$0<r_k<\frac{3}{2}$	$\Omega<\frac{1+\eta}{\eta-1}\Omega_0$	saddle	center	nonexistence	L-J
	$\Omega>\frac{1+\eta}{\eta-1}\Omega_0$	center	center	saddle	
$r_k=\frac{3}{2}$		saddle	center	nonexistence	Toda and Morse
$\frac{3}{2}<r_k<\frac{9}{4}$	$\Omega<\frac{1+\eta}{1-\eta}\Omega_0$	saddle	center	nonexistence	B-M-C
	$\Omega>\frac{1+\eta}{1-\eta}\Omega_0$	saddle	saddle	center	

C. Coupled soliton solutions for small band gap (II)

To solve Eqs. (50)–(52), we integrate Eqs. (50) and (52) with respect to ξ_n once, and make the transformation $u=\epsilon F_{10}$, $w=\epsilon F_{11}\exp\{i[K_3d/(\overline{m\omega})]t\}$, and $w_1=\epsilon^2F_{21}$. Then we have

$$\frac{\partial u}{\partial x_n}=-\frac{16K_3}{K_2d}|w|^2+C_0, \tag{113}$$

$$i\frac{\partial w}{\partial t}+\frac{v_2^2}{2\bar{\omega}}\frac{\partial^2 w}{\partial x_n^2}+\frac{12K_4}{\overline{m\omega}}\left(r_k-\frac{1}{2}\right)|w|^2w=0, \tag{114}$$

$$w_1=\frac{d}{4}\frac{\partial w}{\partial x_n}-is_1\frac{\Delta}{2d}\int w(x_n,t)dx_n+C_1, \tag{115}$$

when we return to the original variables. Here x_n-v_2t again with $v_2=K_2d/(2\overline{m\omega})$. C_0 and C_1 are two integration constants. C_1 may be taken as zero since it represents a translation of the system as a whole.

Equation (114) is the NLS equation, which has been intensively studied. For $r_k<1/2$ (the Lennard-Jones potential applies in this case), we have the single-soliton solution

$$w=\frac{v_2}{\sqrt{\bar{\omega}A_0}}\eta_0\,\mathrm{sech}(\eta_0x_n)\exp[i(\tfrac{1}{2}\eta_0^2t-\phi_0)], \tag{116}$$

with $A_0=12K_4(1/2-r_k)/(\overline{m\omega})$, where η_0 and ϕ_0 are two arbitrary constants. The dc component can be obtained by integrating Eq. (113):

$$u=\frac{16K_3v_2^2}{K_2d\bar{\omega}A_0}\eta_0\tanh(\eta_0x_n)+C_0x_n. \tag{117}$$

The constant C_0 should vanish for the excitation with finite energy. Using Eq. (115) one gets the companion component

$$w_1=\frac{v_2}{\sqrt{\bar{\omega}A_0}}\left(-\frac{d}{4}\eta_0^2\,\mathrm{sech}(\eta_0x_n)\tanh(\eta_0x_n)-is_1\frac{\Delta}{2d}\arctan[\sinh(\eta_0x_n)]\right)\exp[i[\tfrac{1}{2}\eta_0^2t-\phi_0)]. \tag{118}$$

From Eqs. (116)–(118) we see that the principal component of the lattice vibration, w, is an envelope soliton and the dc background, u, is a kink; while the companion component, w_1, consists of two parts, an asymmetric envelope soliton with two extrema and an envelope kink.

If $r_k>1/2$ (the potentials of Toda, Morse, and Born-Mayer-Coulomb belong to this case), we can also solve Eqs. (113) and (115). The result shows that both w and u are kinks. However, when solving for w_1 from Eq. (115), there is a divergence unless $\Delta=0$. Thus we conclude that, for $r_k>1/2$, these solutions are not physically meaningful and hence not allowed. This is due to the cubic nonlinearity as for symmetric potentials $r_k=0$ the solutions (116)–(118) are always valid.

IV. DISCUSSION AND SUMMARY

Based on an extended QDA we have *analytically* investigated the dynamics of coupled gap solitons in diatomic lattices with cubic and quartic intersite nonlinearities. A general scheme is provided for deriving several types of coupled-mode equations, without using the rotating-wave approximation or any ansatz for the solutions. The relation between different theoretical approaches existing in the literature for the gap soliton dynamics in diatomic lattices is made clear. Our results also show that two parameters of the system, i.e., the force-constant ratio $r_k=K_3^2/(K_2K_4)$ and the mass ratio $r_m=m/M$, are of crucial importance for making the asymptotic expansions and characterizing the gap solitons and their coupling. Furthermore, some exact coupled soliton solutions for the coupled-mode equations given in Eqs. (23)–(25) (for the wide band gap) and Eqs. (38)–(39) and (50)–(52) (for the small band gap), which have couplings to mean field (dc) components, are explicitly presented. Effects due

TABLE III. The envelope equations for different widths of the band gap of the phonon spectrum and different spatial-temporal extents of the excitation in diatomic lattices. The parameters α, β, and γ are the exponents expressed in Eq. (12).

Gap width	γ	α	β	Envelope equations
Wide	0	2	1	CNLSM Eqs. (23)–(25)
Intermediate	1			linear dispersive Eqs. (54), (55)
Small	2	2	2	Eqs. (38), (39)
		2	1	Eqs. (50)–(52)
Negligible	$\geqslant 3$	2	1	Eqs. (50), (51)

to the cubic nonlinearity, in particular, types of coupled gap solitons that are absent in the case of symmetric potentials, are discussed in detail.

We have shown that the relative order of magnitude of different small parameters appearing in the problem is very important for making an asymptotic expansion. Different relative orders require different spatial-temporal scalings, and hence result in different envelope equations. For the dynamics of a gap soliton excitation in diatomic lattices, these smallness parameters include the amplitude, the spatial-temporal extent of the excitation, and the band gap width of the phonon spectrum if the force constants K_j $(j=2,3,4)$ are of order of unity. In our problem, these relative orders of magnitude are expressed by the exponents α, β, and γ, given in Eq. (12). By choosing different values of α, β, and γ, and based on the QDA, we have arrived at several different types of coupled-mode equations, i.e., the CNLSM equations (23)–(25), the generalized coupled-mode equations (38) and (39) [or (41) and (42)], and Eqs. (50)–(52). In Table III, we have summarized results obtained in Secs. II B–II D. We note that, in the context of nonlinear optics, such a systematic procedure for deriving the coupled-mode equation and the nonlinear Schrödinger equation has been considered [29].

Realistic interatomic interaction potentials, like the Lennard-Jones, Toda, Morse, and Born-Mayer-Coulomb potentials, are asymmetric and hence display strong cubic nonlinearity. This shows the interest of considering its influence on gap soliton dynamics. Another parameter, i.e., the force-constant ratio r_k, is thus introduced into the system and we see that it plays a very significant role. It helps the production of the mean (dc) fields, which are coupled to ac components, together with the appearance of some other sum- and difference-frequency components in higher orders. In consequence, the coupled-mode equations are modified by the mean fields, a result of much interest in the context of nonlinear optics [26,27]. The parameter r_k is also important for controlling and characterizing the coupled gap solitons. In addition, from the exact soliton solutions given in Secs. III A and III B, we see that, relative to the case with no cubic nonlinearity, nonvanishing r_k yields many additional types of coupled gap solitons in the system.

The theoretical scheme presented here is not limited only to 1D diatomic lattices with nonlinear intersite potentials. The application to on-site potentials is straightforward. A generalization to higher dimensional and multiatomic lattice systems also seems feasible with reasonable effort.

ACKNOWLEDGMENTS

The authors wish to express their gratitude to O. M. Braun, Y. S. Kivshar, and V. V. Konotop for useful discussions and suggestions. This work was supported by the Natural Science Foundation of China, the Program for Training Talents of the Ministry of Education of China, the Hong Kong Research Grants Council (RGC), a Hong Kong Baptist University Faculty Research Grant (FRG), and the Spanish Ministry of Education and Culture under Grant No. PB96-599.

APPENDIX A

The expressions for $P_{n,n}^{(j)}$ and $Q_{n,n}^{(j)}$ $(j=1,2,3,\dots)$ used in Sec. II C are defined by

$$P_{n,n}^{(1)}=0, \tag{A1}$$

$$P_{n,n}^{(2)}=K_3(w_{n,n}^{(1)}-v_{n,n}^{(1)})^2-K_3(w_{n,n-1}^{(1)}-v_{n,n}^{(1)})^2, \tag{A2}$$

$$\begin{aligned}P_{n,n}^{(3)}=&-2\bar{m}\frac{\partial^2}{\partial t\partial\tau}v_{n,n}^{(1)}+\bar{m}\Delta\frac{\partial^2}{\partial t^2}v_{n,n}^{(1)}-K_2d\frac{\partial}{\partial\xi_n}w_{n,n-1}^{(1)}\\&+2K_3(w_{n,n}^{(1)}-v_{n,n}^{(1)})(w_{n,n}^{(2)}-v_{n,n}^{(2)})-2K_3(w_{n,n-1}^{(1)}-v_{n,n}^{(1)})\\&\times(w_{n,n-1}^{(2)}-v_{n,n}^{(2)})+K_4(w_{n,n}^{(1)}-v_{n,n}^{(1)})^3+K_4(w_{n,n-1}^{(1)}\\&-v_{n,n}^{(1)})^3,\end{aligned} \tag{A3}$$

$\dots,$

and

$$Q_{n,n}^{(1)}=0, \tag{A4}$$

$$Q_{n,n}^{(2)}=-K_3(v_{n,n}^{(1)}-w_{n,n}^{(1)})^2+K_3(v_{n,n+1}^{(1)}-w_{n,n}^{(1)})^2, \tag{A5}$$

$$\begin{aligned}Q_{n,n}^{(3)}=&-2\bar{m}\frac{\partial^2}{\partial t\partial\tau}w_{n,n}^{(1)}-\bar{m}\Delta\frac{\partial^2}{\partial t^2}w_{n,n}^{(1)}+K_2d\frac{\partial}{\partial\xi_n}v_{n,n+1}^{(1)}\\&-2K_3(v_{n,n}^{(1)}-w_{n,n}^{(1)})(v_{n,n}^{(2)}-w_{n,n}^{(2)})+2K_3(v_{n,n+1}^{(1)}-w_{n,n}^{(1)})\\&\times(v_{n,n+1}^{(2)}-w_{n,n}^{(2)})+K_4(v_{n,n}^{(1)}-w_{n,n}^{(1)})^3+K_4(v_{n,n+1}^{(1)}\\&-w_{n,n}^{(1)})^3,\end{aligned} \tag{A6}$$

$\dots,$

APPENDIX B

The expressions for $R_{n,n}^{(j)}$ and $S_{n,n}^{(j)}$ $(j=1,2,3,\dots)$ mentioned in Sec. II D are given by

$$R_{n,n}^{(1)}=0, \tag{B1}$$

$$\begin{aligned}R_{n,n}^{(2)}=&2\bar{m}\lambda\frac{\partial^2}{\partial t\partial\xi_n}v_{n,n}^{(1)}-K_2d\frac{\partial}{\partial\xi_n}w_{n,n-1}^{(1)}+K_3(w_{n,n}^{(1)}-v_{n,n}^{(1)})^2\\&-K_3(w_{n,n-1}^{(1)}-v_{n,n}^{(1)})^2,\end{aligned} \tag{B2}$$

$$R^{(3)}_{n,n}=2\overline{m}\lambda\frac{\partial^2}{\partial t\partial\xi_n}v^{(2)}_{n,n}-\overline{m}\left(2\frac{\partial^2}{\partial t\partial\tau}+\lambda^2\frac{\partial^2}{\partial\xi_n^2}\right)v^{(1)}_{n,n}+\overline{m}\Delta\frac{\partial^2}{\partial t^2}v^{(1)}_{n,n}+K_2\left(-d\frac{\partial}{\partial\xi_n}w^{(2)}_{n,n-1}+\frac{d^2}{2}\frac{\partial^2}{\partial\xi_n^2}w^{(1)}_{n,n-1}\right)+2K_3(w^{(1)}_{n,n}-v^{(1)}_{n,n})(w^{(2)}_{n,n}-v^{(2)}_{n,n})-2K_3(w^{(1)}_{n,n-1}-v^{(1)}_{n,n})\left(w^{(2)}_{n,n-1}-v^{(2)}_{n,n}-d\frac{\partial}{\partial\xi_n}w^{(1)}_{n,n-1}\right)+K_4(w^{(1)}_{n,n}-v^{(1)}_{n,n})^3+K_4(w^{(1)}_{n,n-1}-v^{(1)}_{n,n})^3, \tag{B3}$$

. . . ,

and

$$S^{(1)}_{n,n}=0, \tag{B4}$$

$$R^{(2)}_{n,n}=2\overline{m}\lambda\frac{\partial^2}{\partial t\partial\xi_n}w^{(1)}_{n,n}+K_2d\frac{\partial}{\partial\xi_n}v^{(1)}_{n,n+1}-K_3(v^{(1)}_{n,n}-w^{(1)}_{n,n})^2+K_3(v^{(1)}_{n,n+1}-w^{(1)}_{n,n})^2, \tag{B5}$$

$$R^{(3)}_{n,n}=2\overline{m}\lambda\frac{\partial^2}{\partial t\partial\xi_n}w^{(2)}_{n,n}-\overline{m}\left(2\frac{\partial^2}{\partial t\partial\tau}+\lambda^2\frac{\partial^2}{\partial\xi_n^2}\right)w^{(1)}_{n,n}-\overline{m}\Delta\frac{\partial^2}{\partial t^2}w^{(1)}_{n,n}+K_2\left(d\frac{\partial}{\partial\xi_n}v^{(2)}_{n,n+1}+\frac{d^2}{2}\frac{\partial^2}{\partial\xi_n^2}v^{(1)}_{n,n+1}\right)-2K_3(v^{(1)}_{n,n}-w^{(1)}_{n,n})(v^{(2)}_{n,n}-w^{(2)}_{n,n})+2K_3(v^{(1)}_{n,n+1}-w^{(1)}_{n,n})\times\left(v^{(2)}_{n,n+1}-w^{(2)}_{n,n}+d\frac{\partial}{\partial\xi_n}v^{(1)}_{n,n+1}\right)+K_4(v^{(1)}_{n,n}-w^{(1)}_{n,n})^3+K_4(v^{(1)}_{n,n+1}-w^{(1)}_{n,n})^3, \tag{B6}$$

. . . .

[1] E. Fermi, J. Pasta, and S. Ulam, Los Alamos National Laboratory Report LA1940, 1955 (unpublished). Also in *Collected Papers of Enrico Fermi* (Univ. Chicago Press, Chicago, 1962), Vol. 2, p. 978.
[2] Zhu-Pei Shi, Guoxiang Huang, and Ruibao Tao, Int. J. Mod. Phys. B **5**, 2237 (1991).
[3] Y.S. Kivshar and N. Flytzanis, Phys. Rev. A **46**, 7972 (1992).
[4] S.A. Kiselev, S.R. Bickham, and A.J. Sievers, Phys. Rev. B **48**, 13 508 (1993); **50**, 9153 (1994).
[5] Guoxiang Huang, Phys. Rev. B **51**, 12 347 (1995).
[6] M. Aoki and S. Takeno, J. Phys. Soc. Jpn. **64**, 809 (1995).
[7] D. Bonart, A.P. Mayer, and U. Schröder, Phys. Rev. Lett. **75**, 870 (1995); Phys. Rev. B **51**, 13 739 (1995).
[8] D. Bonart, T. Rössler, and J.B. Page, Phys. Rev. B **55**, 8829 (1997).
[9] J.N. Teixeira and A.A. Maradudin, Phys. Lett. A **205**, 349 (1995).
[10] A. Franchini, V. Bortolani, and R.F. Wallis, Phys. Rev. B **53**, 5420 (1996).
[11] V.V. Konotop, Phys. Rev. E **53**, 2843 (1996), Sec. III.
[12] S.A. Kiselev and A.J. Sievers, Phys. Rev. B **55**, 5755 (1997).
[13] Guoxiang Huang and Bambi Hu, Phys. Rev. B **57**, 5746 (1998).
[14] S. Jiménez and V.V. Konotop, Phys. Rev. B **60**, 6465 (1999).
[15] W. Chen and D.L. Mills, Phys. Rev. Lett. **58**, 160 (1987).
[16] Sen-yue Lou and Guoxiang Huang, Mod. Phys. Lett. A **9**, 1231 (1995).
[17] Sen-yue Lou, Jun Yu, Ji Lin, and Guoxiang Huang, Chin. Phys. Lett. **12**, 400 (1995).
[18] Ji Lin, Yong Li, Guoxiang Huang, and Sen-yue Lou, Chin. Sci. Bull. **4**, 120 (1997).
[19] O.A. Chubykalo, A.S. Kovalev, and O.V. Usatenko, Phys. Rev. B **47**, 3153 (1993).
[20] Y.S. Kivshar, O.A. Chubykalo, O.V. Usatenko, and D.V. Grinyoff, Int. J. Mod. Phys. B **9**, 2963 (1996).
[21] A.S. Kovalev, O.V. Usatenko, and A.V. Gorbatch, Phys. Rev. E **60**, 2309 (1999).
[22] D.L. Mills and S.E. Trullinger, Phys. Rev. B **36**, 947 (1987). Similar coupled mode equations were also obtained earlier by H.G. Winful *et al.*, Appl. Phys. Lett. **35**, 379 (1979); **40**, 298 (1982).
[23] A. Jeffery and T. Kawahawa, *Asymptotic Method in Nonlinear Wave Theory* (Pitman, London, 1982).
[24] M.C. Cross and P.C. Hohenberg, Rev. Mod. Phys. **65**, 851 (1993).
[25] A. Tsurui, Prog. Theor. Phys. **48**, 1196 (1972).
[26] M.J. Ablowitz, G. Biondini, and S. Blair, Phys. Lett. A **236**, 520 (1997).
[27] T. Iizuka and Y.S. Kivshar, Phys. Rev. E **59**, 7148 (1999).
[28] C.M. de Sterke, Phys. Rev. E **48**, 4136 (1993).
[29] C.M. de Sterke, D.G. Salinas, and J.E. Sipe, Phys. Rev. E **54**, 1969 (1996).
[30] Guoxiang Huang, Zhu-Pei Shi, and Zaixin Xu, Phys. Rev. B **47**, 14 561 (1993).
[31] A.V. Buryak, Y.S. Kivshar, and D.F. Parker, Phys. Lett. A **215**, 57 (1996), and references therein.
[32] Guoxiang Huang, Peiqing Tong, and Bambi Hu, J. Phys.: Condens. Matter **11**, 2759 (1999).